Dyes and Pigments 95 (2012) 174–179

Contents lists available at SciVerse ScienceDirect

Dyes and Pigments

journal homepage: www.elsevier.com/locate/dyepig

Zn^{2+}-selective fluorescent turn-on chemosensor based on terpyridine-substituted siloles

Shouchun Yin [a], Jing Zhang [a], Haike Feng [a], Zujin Zhao [a], Liwen Xu [b], Huayu Qiu [a,b,*], Benzhong Tang [c]

[a] College of Material, Chemistry and Chemical Engineering, Hangzhou Normal University, Hangzhou 310036, China
[b] Key Laboratory of Organosilicon Chemistry and Material Technology of Ministry of Education, Hangzhou Normal University, Hangzhou 310012, China
[c] Department of Chemistry and State Key Laboratory of Molecular Neuroscience, The Hong Kong University of Science & Technology, Clear Water Bay, Kowloon, Hong Kong, China

ARTICLE INFO

Article history:
Received 15 March 2012
Received in revised form
16 April 2012
Accepted 17 April 2012
Available online 25 April 2012

Keywords:
Siloles
Terpyridine
Fluorescent sensor
Zinc (II)
Aggregation-induced emission
Spectroscopic properties

ABSTRACT

Two terpyridine-containing siloles (**1** and **2**) have been synthesized and their optical and metal sensing properties have been investigated in this work. **1** and **2** display a high selectivity for Zn^{2+} in comparison with alkali and alkaline earth metal ions (Na^+, K^+, Mg^{2+}, Ca^{2+}) and other transition metal ions (Ba^{2+}, Zn^{2+}, Fe^{2+}, Pb^{2+}, Ni^{2+}, Co^{2+}, Hg^{2+}, Ag^+) upon excitation at 380 nm in THF. As being chemosensor, **1** with two terpyridine groups at both ends shows better Zn^{2+} sensing properties than **2** containing only one terpyridine group at end due to the formation of a metal–organic coordination oligomer or polymer.

1. Introduction

In the past decade, the development of fluorescent chemosensors with high selectivity and sensitivity has been a great interest field in supramolecular chemistry [1]. Zn^{2+} is the second most abundant transition metal ion in the human system after iron, which plays an important role in various biological processes, such as enzyme regulation, gene expression, neural signal transduction and protein synthesis [2,3,4]. However, if unregulated, Zn^{2+} can cause many severe diseases, such as Alzheimer's disease, Parkinson's disease, amyotrophic lateral sclerosis, hypoxia–ischemia and epilepsy [5,6,7]. Meanwhile, excessive Zn^{2+} makes water smelly and muddy, which is harmful to the environment [8]. Thus, the development of an efficient Zn^{2+}-selective fluorescent sensor is important for the fundamental research and biological application [9,10,11].

Siloles are a class of particularly interesting molecules that possess low-lying LUMO levels and high electron affinity arising from the orbital interaction of the σ* orbital of the silylene moiety with the π* orbital of the butadiene fragment [12,13]. Siloles also show intriguing aggregation-induced emission (AIE) characteristic, first reported by Tang and co-workers [14]. Propeller-like silole molecules are almost nonluminescent in solutions but become highly emissive when aggregated in poor solvents or in solid state. Therefore, due to the excellent photophysical and electronic properties, siloles have been widely used as organic electroluminescent devices, organic solar cells, and chemosensors for explosive detection and ion monitoring [15–29].

It is well known that terpyridine has a strong and directed metal coordination capacity [30]. We connected the terpyridine moiety covalently with the silole core in order to endow silole with metal chelating properties. Here, we report the synthesis and characterization of two terpyridine end-capped siloles, 1,1-dimethyl-3,4-diphenyl-2,5-bis(4′-biphenyl-2,2′:6′,2″-terpyridine) silole (**1**) and 1,1-dimethyl-3,4-diphenyl-2-(4-biphenyl-2,2′:6′,2″-terpyridine)-5-(p-bromophenyl) silole (**2**). Their photophysical properties and potential applications as metal ion sensors have been investigated. **1** and **2** display a high selectivity for Zn^{2+} in comparison with all other test metal ions upon excitation at 380 nm in THF. As being chemosensor, **1** with two terpyridine groups at both ends shows better Zn^{2+} sensing properties than **2** containing one terpyridine group due to the formation of metal–organic coordination oligomer or polymer.

* Corresponding author. College of Material, Chemistry and Chemical Engineering, Hangzhou Normal University, Hangzhou 310036, China. Tel.: +86 571 28867898; fax: +86 571 28867899.
E-mail address: huayuqiu@gmail.com (H. Qiu).

0143-7208/$ – see front matter © 2012 Elsevier Ltd. All rights reserved.
doi:10.1016/j.dyepig.2012.04.007

2. Experimental

2.1. Materials

1,1-Dimethyl-3,4-diphenyl-2,5-bis(4-bromophenyl)silole was synthesized according to literature procedures [31]. 4-Bromobenzaldehyde, 2-acetylpyridine, 3,4-dimethoxyphenylboronic acid, bis(pinacolato)diboron, dry dimethyl sulfoxide (DMSO), [1,1′-bis(diphenylphosphino)ferrocene]dichloropalladium(II) [$Pd(dppf)Cl_2$], and tetrakis(triphenylphosphine)palladium(0) [$Pd(PPh_3)_4$] were purchased from Acros and used without further purification. Tetrahydrofuran (THF) was distilled from sodium prior to use. The metal salts [$AgClO_4$, $Ba(ClO_4)_2$, $Ca(ClO_4)_2$, $Co(ClO_4)_2$, $Cu(ClO_4)_2\cdot 6H_2O$, $FeCl_2\cdot 4H_2O$, $Hg(ClO_4)_2$, $KClO_4$, $Mg(ClO_4)_2$ $NaClO_4$, $Ni(ClO_4)_2\cdot 6H_2O$, $Pb(ClO_4)_2\cdot 3H_2O$ and $Zn(ClO_4)_2$] were purchased from Aldrich.

2.2. Instrumentation

^1H and ^{13}C NMR spectra were recorded at room temperature on a Bruker Avance 400 operating at a frequency of 400 MHz for ^1H and 100 MHz for ^{13}C. Melting points were taken on a Beijing Taike X-5 melting point instrument. Mass spectra were recorded on a Hewlett-Packard 5989 A mass spectrometer (ESI mode) and Bruker Daltonics' micrOTOF-Q II 10324 (MALDI-TOF MS).

UV–vis absorption spectra were recorded on a Perkin Elmer Lambda 40 UV–vis spectrophotometer. Corrected steady-state excitation and emission spectra were obtained using a HITACHI F-2700 Fluorescence Spectrophotometer. Relative quantum yields were obtained by comparing the areas under the corrected emission spectra of sample and fluorescence standard. Coumarin I in ethanol (λ_{ex} = 380 nm, Φ_f = 0.64) was used as fluorescence standard. All spectra were recorded at 25 °C using undegassed samples.

2.3. Synthesis

2.3.1. 4′-(p-Bromophenyl)-2,2′:6′,2″-terpyridine (**6**)

To 4-bromobenzaldehyde (1.0 g, 5.40 mmol) in 120 mL CH_3OH was added 2-acetylpyridine (1.3 g, 10.80 mmol), NaOH (0.22 g, 5.4 mmol) and 30 mL concentrated NH_4OH. The reaction mixture was refluxed for 72 h, and then stirred at room temperature for another 3 h. The formed slight yellow precipitate was filtered and washed sequentially with H_2O and CH_3OH. White powder could be obtained after recrystallization from EtOH (1.8 g, 88% yield). M. p. = 155–157 °C. ^1H NMR (400 MHz, $CDCl_3$) δ (ppm): 8.71 (d, J = 4.2 Hz, 2H), 8.66 (s, 2H), 8.63 (d, J = 8.6 Hz, 2H), 7.86 (m, 2H), 7.75 (d, J = 8.6 Hz, 2H), 7.61 (d, J = 8.6 Hz, 2H), 7.35 (m, 2H). ^{13}C NMR (100 MHz, $CDCl_3$) δ (ppm): 156.0, 149.1, 149.0, 137.4, 136.9, 132.1, 128.9, 123.9, 123.4, 121.3, 118.5.

2.3.2. 4′-(p-Pinacolatoboronphenyl)-2,2′:6′,2″-terpyridine (**5**)

774 mg **6** (2 mmol), 533 mg bis(pinacolato)diboron (2.1 mmol), 50 mg $Pd(dppf)Cl_2$ (0.06 mmol) and 402 mg KOAc (6 mmol) were added into 5 mL of dry and degassed DMSO, and then flushed with nitrogen. The mixture was stirred at 80 °C for 6 h under nitrogen. Then 50 mL of toluene was added and washed with water (3 × 150 mL) to remove DMSO from the toluene layer. The toluene layer was dried over $MgSO_4$ and the solvent was evaporated under reduced pressure to give a white solid (348 mg, 40% yield). M. p. = 187–194 °C. ^1H NMR (400 MHz, $CDCl_3$) δ (ppm): 8.76 (s, 2H), 8.75 (d, J = 4.8 Hz, 2H), 8.65 (d, J = 7.9 Hz, 2H), 7.97 (d, J = 8.4 Hz, 2H), 7.94 (d, J = 8.4 Hz, 2H), 7.87 (d, J = 7.9 Hz, 2H), 7.35 (m, 2H), 1.38 (s, 6H).

2.3.3. 1,1-Dimethyl-3,4-diphenyl-2,5-bis(4′-biphenyl-2,2′:6′,2″-terpyridine) silole (**1**)

570 mg (1.0 mmol) 1,1-dimethyl-3,4-diphenyl-2,5-bis(4-bromophenyl)silole (**4**), 435 mg (1.0 mmol) **5** and 138 mg K_2CO_3 (1.0 mmol) were dissolved in 25 mL of THF and 5 mL of H_2O under argon. To this solution 115 mg (0.1 mmol) $Pd(PPh_3)_4$ were added. The reaction mixture was refluxed for 72 h. After cooling to room temperature, the precipitate was filtered, and dissolved in excess amount of CH_2Cl_2 (500 mL). The solution was then washed with aqueous KOH solution (2%) and water. The organic layer was separated and dried over $MgSO_4$. After filtration, the solvent was evaporated under reduced pressure to give yellow solid **1** (180 mg, 35% yield). M. p. = 335–339 °C. ^1H NMR (400 MHz, $CDCl_3$) δ (ppm): 8.76 (s, 4H), 8.72 (d, 4H), 8.66 (d, J = 8.0 Hz, 4H), 7.95 (d, J = 8.0 Hz, 4H), 7.85 (d, J = 6.8 Hz, 4H), 7.69 (d, J = 8.0 Hz, 5H), 7.47 (d, J = 7.6 Hz, 4H), 7.32 (d, J = 5.2 Hz, 5H), 7.25 (m, 2H), 7.08 (m, 4H), 6.92 (m, 4H), 0.59 (s, 6H). ^{13}C NMR (100 MHz, $CDCl_3$) δ (ppm): 156.1, 155.8, 154.6, 154.0, 150.0, 149.0, 141.3, 141.2, 140.5, 138.9, 138.7, 138.6, 138.3, 137.2, 136.8, 131.0, 130.3, 129.8, 129.3, 127.5, 127.1, 126.5, 126.4, 123.8, 121.3, 119.4, 118.5, −3.8. MALDI-TOF MS: calcd. for $C_{72}H_{52}N_6Si$ 1029.4098, found 1029.4095.

2.3.4. 1,1-Dimethyl-3,4-diphenyl-2-(4-biphenyl-2,2′:6′,2″-terpyridine)-5-(p-bromophenyl) silole (**3**)

This compound was synthesized by analogous procedures described for **1**, from 285 mg (0.5 mmol) **4**, 218 mg (0.5 mmol) **5**, 69 mg K_2CO_3 (0.5 mmol), and 58 mg (0.05 mmol) $Pd(PPh_3)_4$. Purification was performed by chromatography on silica gel with a mixture of petroleum ether and ethyl acetate (4:1, v/v) to give a yellow solid (228 mg, 57% yield). M. p. = 292–296 °C. ^1H NMR (400 MHz, $CDCl_3$) δ (ppm): 8.78 (s, 2H), 8.74 (d, J = 4.0 Hz, 2H), 8.69 (d, J = 8.0 Hz, 2H), 7.96 (d, J = 8.4 Hz, 2H), 7.89 (m, 2H), 7.70 (d, J = 8.4 Hz, 2H), 7.46 (d, J = 8.4 Hz, 2H), 7.36 (t, J = 6.8 Hz, 2H), 7.25 (d, J = 8.0 Hz, 2H), 7.04 (m, 8H), 6.86 (m, 2H), 6.80 (d, J = 8.0 Hz, 4H), 0.52 (s, 6H). ESI-MS: m/z 800.55 $[M + H]^+$.

2.3.5. 1,1-Dimethyl-3,4-diphenyl-2-(4-biphenyl-2,2′:6′,2″-terpyridine)-5-(p-bromophenyl) silole (**2**)

This compound was synthesized by analogous procedures described for **1**, from 200 mg (0.25 mmol) **3**, 91 mg (0.5 mmol) 3,4-dimethoxyphenylboronic acid, 35 mg K_2CO_3 (0.25 mmol), and 29 mg (0.025 mmol) $Pd(PPh_3)_4$. Purification was performed by chromatography on silica gel with a mixture of petroleum ether and ethyl acetate (4:1, v/v) to give a yellow solid (139 mg, 65% yield). M. p. = 315–318 °C. ^1H NMR (400 MHz, $CDCl_3$) δ (ppm): 8.83 (s, 2H), 8.77 (d, J = 4.4 Hz, 2H), 8.72 (d, J = 7.6 Hz, 2H), 8.01 (d, J = 8.0 Hz, 2H), 7.94 (t, J = 7.6 Hz, 2H), 7.72 (d, J = 8.0 Hz, 2H), 7.47 (d, J = 8.4 Hz, 2H), 7.40 (t, J = 6.0 Hz, 2H), 7.35 (d, J = 8.4 Hz, 2H), 7.26 (m, 3H), 7.06 (m, 8H), 7.01 (d, J = 8.4 Hz, 2H), 6.80 (m, 4H), 3.93 (s, 3H), 3.91 (s, 3H), 0.57 (s, 6H). ESI-MS: m/z 858.55 $[M + H]^+$.

3. Results and discussion

3.1. Synthesis

Silole derivate **1** with two terpyridine functional groups at both ends (1,1-dimethyl-3,4-diphenyl-2,5-bis(4′-biphenyl-2,2′:6′,2″-terpyridine) silole) was synthesized according to the synthetic route shown in Scheme 1. In the presence of NaOH and concentrated NH_4OH, 4-bromobenzaldehyde was reacted with 2-acetylpyridine to get **6**. By Miyaura coupling reaction the bromo group of **6** was transferred into pinacolatoboron group at the presence of $Pd(dppf)_2Cl_2$ as catalyst. The Suzuki coupling of **4** and **5** with $Pd(PPh_3)_4$ as catalyst afforded ditopic ligand **1** and **3** in moderate yields of 35% and 57%, respectively. Although we can obtain **1** and **3**

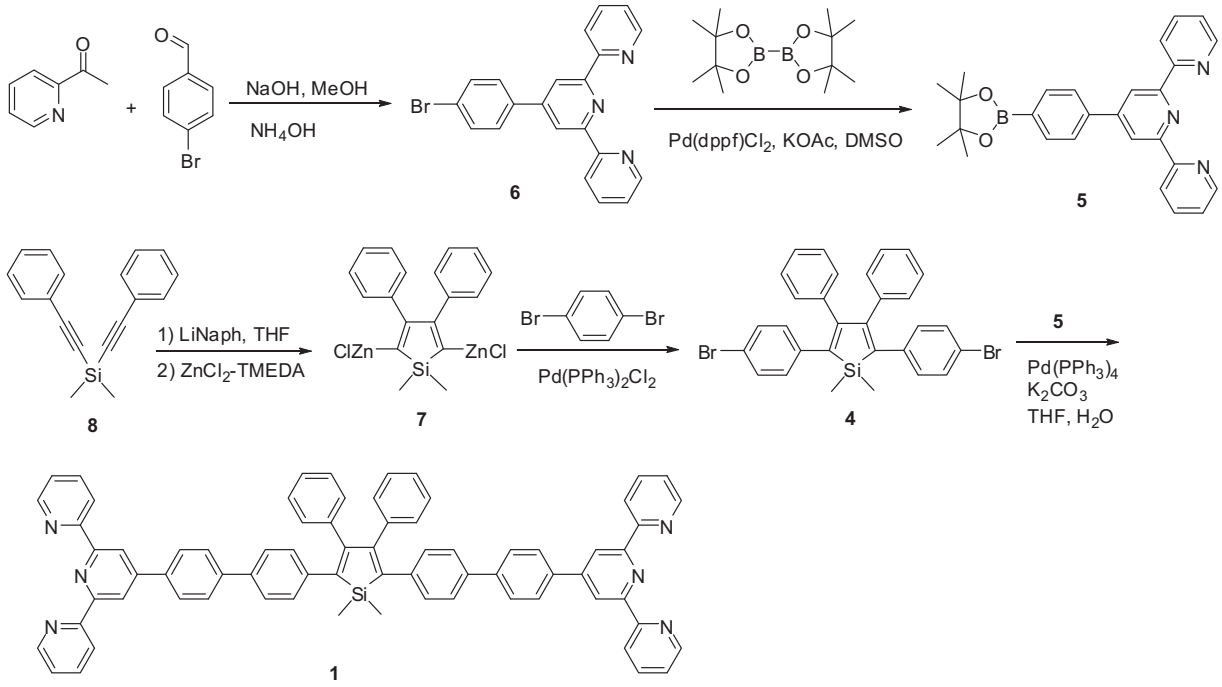

Scheme 1. Synthetic route to **1**.

simultaneously by one-pot Suzuki coupling reaction of **4** and **5**, the separation of the products is very difficult and cumbersome, and it is not easy to get the compounds pure enough for NMR spectroscopic characterization. Here, an excess amount of **4** was used and the reaction time was elongated to make sure that **5** was reacted completely during the synthetic procedure of **1**, which facilitates the separation of the desired products. On the other hand, an equal equivalent of **4** and **5** in a short reaction time yields intermediate **3** that reacts with 3,4-dimethoxyphenylboronic acid to afford **2** for comparison (Scheme 2). The reaction intermediates and final products were fully characterized by NMR and Mass spectroscopy and satisfactory data corresponding to their structures are obtained. **1** and **2** are soluble in THF, CH_3CN and DMSO, and slightly soluble in C_2H_5OH and CH_3OH.

3.2. Spectral characteristics

As terpyridine is a well-known metal chelating unit, we wondered if **1** can be used as a chemosensor for metal ions. The photophysical properties of **1** upon addition of several metal cations (Na^+, K^+, Mg^{2+}, Ca^{2+}, Ba^{2+}, Cu^{2+}, Zn^{2+}, Fe^{2+}, Pb^{2+}, Ni^{2+}, Co^{2+}, Hg^{2+}, Ag^+) in THF were investigated by fluorescence spectroscopic measurements and titration studies. Fig. 1 shows the fluorescence response of **1** (1.0×10^{-4} mol/L) to the above mentioned metal cations (1 equiv) measured in THF upon excitation at $\lambda_{ex} = 380$ nm. A THF solution of free **1** shows weak fluorescence peaked at ~500 nm but the intensity is very weak due to the intramolecular rotations of the phenyl rings linked to silole core [25]. In the presence of Na^+, K^+, Mg^{2+}, Ca^{2+} and Ba^{2+}, the fluorescence intensity and the spectral pattern of **1** show no obvious changes. Addition of Cu^{2+}, Fe^{2+}, Pb^{2+}, Ni^{2+}, Co^{2+} and Hg^{2+} to free **1** quenches the light emission, accompanied by a red-shift of ~10 nm. The emission maximum of free **1** further moves to 526 nm, but the emission intensity changes slightly when Ag^+ ions are added. Ag^+ can induce the enhancement of the fluorescence intensity, instead of quenching, by 15% compared with Cu^{2+}, Fe^{2+}, Pb^{2+}, Ni^{2+}, Co^{2+}, Hg^{2+}. Interestingly, when Zn^{2+} ions are added to **1** in THF solution, the fluorescence spectrum of the complex shows

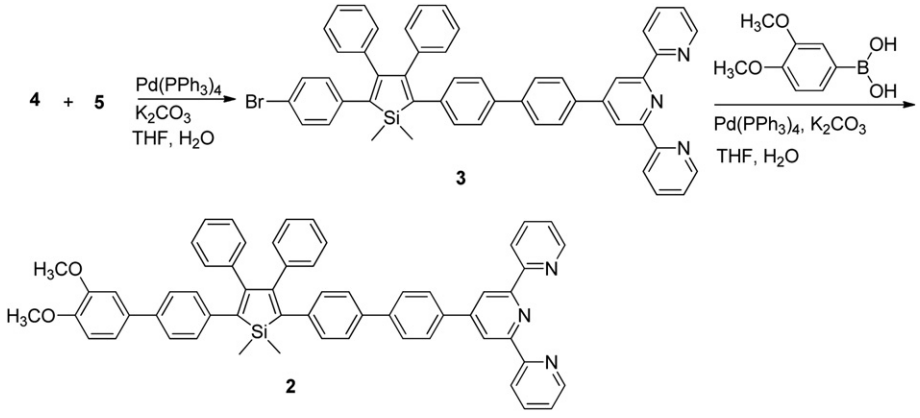

Scheme 2. Synthetic route to **2**.

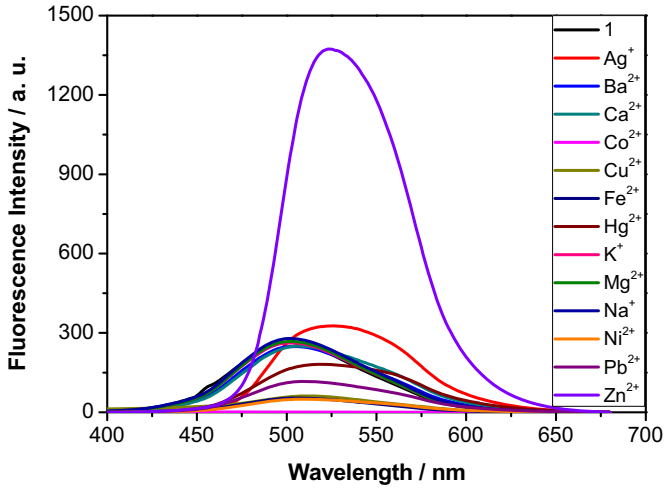

Fig. 1. Fluorescence emission spectra of **1** (1.0×10^{-4} mol/L) upon addition of various metal ions (1 equiv) in THF ($\lambda_{ex} = 380$ nm).

a significant bathochromic shift and the fluorescence intensity exhibits a great enhancement. Chemosensors showing fluorescence enhancement due to metal–ion binding are more sensitive than those exhibiting fluorescence quenching. These observations indicate that **1** can be used as a turn-on chemosensor for Zn^{2+}.

The emission spectra of **2** upon exposure to the above test metal ions are shown in Fig. 2. Similar to **1**, Na^+, K^+, Mg^{2+}, Ca^{2+} and Ba^{2+} exert no effect on the fluorescence of **2** because terpyridine does not coordinate with the above metal ions, and Cu^{2+}, Fe^{2+}, Pb^{2+}, Ni^{2+}, Co^{2+} and Hg^{2+} can efficiently quench the emission of free **2**. Unlike **1**, in the presence of Ag^+, the spectral pattern keeps unchanged but the fluorescence intensity becomes a little weaker. Zn^{2+} can also shift the emission spectrum of **2** bathochromically but the fluorescence intensity has almost no enhancement.

The red-shifts of **1** and **2** upon coordination with Zn^{2+} may be due to intramolecular charge transfer (ICT) effect. Compared to the silole core terpyridine has stronger electron-withdrawing capability. The coordination of **1** or **2** with Zn^{2+} intensifies the electron-withdrawing character of terpyridine, facilitating the occurrence of the ICT process. Thus, the emission of **1** shifts to the longer wavelengths [32] when Zn^{2+} is added. The greatly enhanced emission of **1** upon coordination with Zn^{2+} may be due to the formation of metal–organic coordination polymers or oligomers, where the entangled molecular chains restrict the intramolecular rotation of the silole core to some extent, and thus reduce the nonradiative energy decay. Comparing the structure of **1** with **2**, it can be seen that **1** contains two terpyridine groups at both ends, while **2** has only one terpyridine group at end. Thus, **2** cannot form polymers or oligomers but a 2:1 complex with Zn^{2+}. Direct evidence for the formation of metal–organic coordination oligomers or polymers was obtained from the results of ^{1}H NMR. As shown in Fig. 3, the absorption of the aryl protons of **1** becomes broadened and the characteristic absorption of terpyridine protons at δ 8.76, 8.72, 8.66, 7.47 ppm shifts to a lower field after the coordination of **1** with Zn^{2+}. The formed oligomer or polymer has lower solubility in THF solution and accordingly form aggregates to result in the enhancement of the fluorescence from the silole core in **1** due to the AIE characteristics of the silole core [25]. The formed dimmer can be soluble in THF, so the fluorescence intensity does not increase. This is may be the reason that the fluorescence intensity is greatly enhanced when Zn^{2+} is coordinated with **1**, not **2**. To prove this hypothesis, we added water (poor solvent) into the THF solution of **2** and Zn^{2+}. After addition of water, the fluorescence intensity the complex of **2** and Zn^{2+} is increased. Because **1** displays better properties as chemosensor than **2**, we will focus our investigation on the metal sensing properties of **1** in the following discussion.

The fluorescence titration of **1** in the presence of different Zn^{2+} concentrations was then performed. As shown in Fig. 4, **1** emits weak fluorescence at ~500 nm. After addition of Zn^{2+} into the THF solution, the emission spectra gradually red-shift and the fluorescence intensity increases significantly with the increase of the concentration of Zn^{2+} when excited at 380 nm. The fluorescence quantum yield increases from 0.05 for free **1** to 0.27 for the complex of **1** and Zn^{2+}, correspondingly. The dependence of the emission intensity at 522 nm on the concentration of Zn^{2+} is shown in the inset of Fig. 4. As depicted in the inset of Fig. 4, the fluorescence intensity at 522 nm increases almost linearly with the increase of the concentration of Zn^{2+} in the range of 1.0 equiv of Zn^{2+}, which facilitates the quantitative analysis of Zn^{2+} in THF.

To determine the binding stoichiometry of **1** and Zn^{2+}, Job's method for the emission is employed. The concentrations of **1** and Zn^{2+} are varied, while the sum of the two concentrations is kept constant at 2.0×10^{-4} mol/L. The change of the fluorescence intensity at 522 nm with the concentration ratio of **1** to Zn^{2+} is

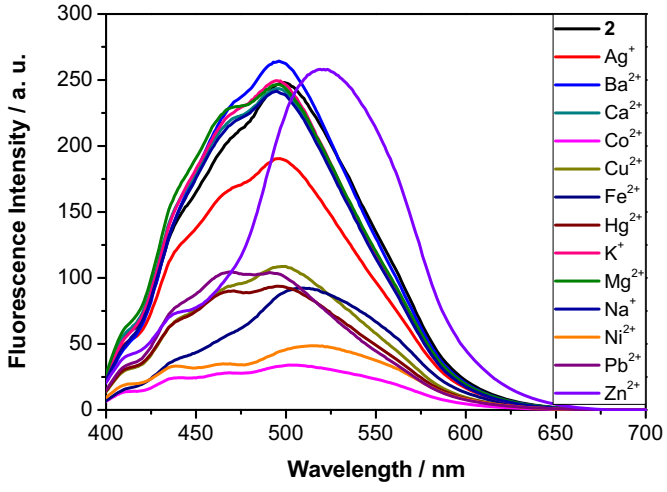

Fig. 2. Fluorescence emission spectra of **2** (1.0×10^{-4} mol/L) upon addition of various metal ions (1 equiv) in THF ($\lambda_{ex} = 380$ nm).

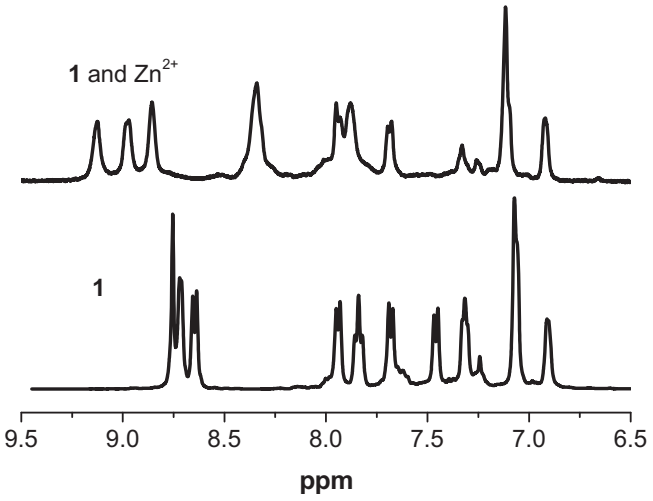

Fig. 3. ^{1}H NMR spectra of **1** and the complex of **1** and Zn^{2+} in chloroform-*d*.

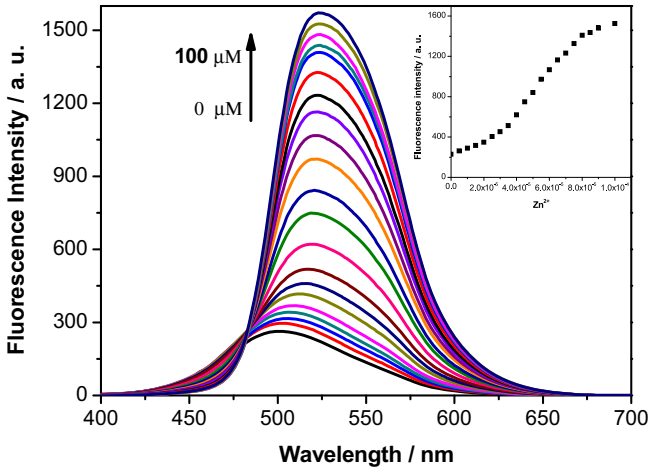

Fig. 4. Fluorescent emission spectra of **1** (1.0×10^{-4} mol/L) upon excitation at 380 nm in the presence of different concentrations of Zn^{2+} (0, 0.05, 0.1, 0.15, 0.2, 0.25, 0.3, 0.35, 0.4, 0.45, 0.5, 0.55, 0.6, 0.65, 0.7, 0.75, 0.8, 0.85, 0.9, 0.95, 1.0 equiv) in THF. Inset: Fluorescence emission intensity of **1** (1.0×10^{-4} mol/L) in THF monitored at 522 nm as a function of Zn^{2+} concentration.

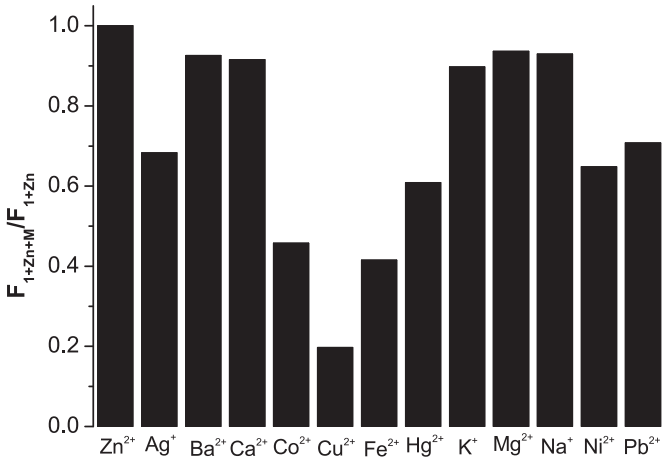

Fig. 6. The relative fluorescence intensity of **1** (1.0×10^{-4} mol/L) containing 1.0 equiv of Zn^{2+} to the selected metal ions (2.0 equiv). F_{1+Zn} and F_{1+Zn+M} denote the fluorescence signals of **1** in the presence of Zn^{2+} only and in the presence of Zn^{2+} as well as the competing ions, respectively. Excitation was at 380 nm and emission was at 522 nm.

shown in Fig. 5. When the molecular fraction of Zn^{2+} is closed to 50%, the complex of **1** and Zn^{2+} exhibited a maximum fluorescence emission at 522 nm. This indicates that a 1:1 stoichiometry is possible for the binding mode of **1** and Zn^{2+}, which is consistent with the binding mode of terpyridine to Zn^{2+} reported in the literature [30,32].

3.3. Selectivity and tolerance of *1* to Zn^{2+} over other metal ions

The selectivity and tolerance of **1** to Zn^{2+} over other metal ions are investigated by measuring the fluorescence response of **1** with Zn^{2+} in the presence of other competitive metal ions. 2.0 Equiv of above mentioned metal ions (2.0×10^{-4} mol/L) was added to 1.0 equiv of the complex of **1** and Zn^{2+} in THF and the fluorescence response (I_{522}) was detected and then compared with that of **1** in THF containing only 1.0 equiv of Zn^{2+}. As shown in Fig. 6, Na^+, K^+, Mg^{2+}, Ca^{2+} and Ba^{2+} exhibit only a small or no interference with the affinity of **1** and Zn^{2+}. However, in the presence of Fe^{2+}, Pb^{2+}, Ni^{2+}, Co^{2+} and Hg^{2+} the fluorescence emission of the coordination of **1** with Zn^{2+} was partly quenched, while Cu^{2+} can almost quench the fluorescence emission of the coordination of **1** with Zn^{2+} due to the paramagnetic properties of Cu^{2+}.

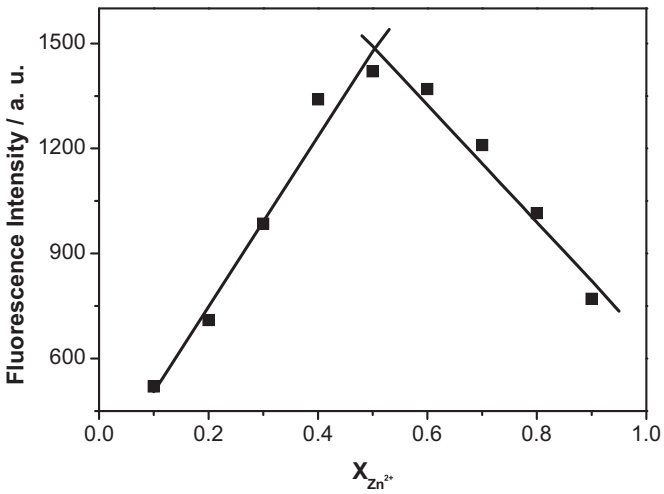

Fig. 5. Job's plot for **1** and Zn^{2+}. The total concentration of **1** and Zn^{2+} was kept at a fixed 2.0×10^{-4} mol/L. The fluorescence intensity was measured at 522 nm.

4. Conclusions

In conclusion, in this work, two terpyridine-containing silole derivatives are synthesized and characterized. The silole derivative **1** with two terpyridine groups can sensitively and selectively detect Zn^{2+} in THF. When Zn^{2+} is added, **1** displays a strong red-shift and a remarkable enhancement of the fluorescence intensity. Thus **1** can be used as a turn-on chemosensor for Zn^{2+}. The future work will focus on the utility of **1** for zinc imaging in live cells.

Acknowledgements

We thank National Natural Science Foundation of China (No. 21074028, 91127032, 21174035, 21104012), Zhejiang Provincial Natural Science Foundation of China (No. Y4100287, Y4110331), Program for Excellent Young Teachers in Hangzhou Normal University (No. HNUEYT 2011-01-019), and the Opening Foundation of Zhejing Provincial Top Key Discipline (No. 20110943) for financial supports.

References

[1] De Silva AP, Gunaratne HQN, Gunnlaugsson T, Huxley TM, McCoy CP, Rademacher JT, et al. Signaling recognition events with fluorescent sensors and switches. Chem Rev 1997;97:1515.
[2] Assaf SY, Chung SH. Release of endogenous Zn^{2+} from brain tissue during activity. Nature 1984;308:734.
[3] Berg JM, Shi Y. The galvanization of biology: a growing appreciation for the roles of zinc. Science 1996;271:1081.
[4] Frederickson CJ, Koh JY, Bush AI. The neurobiology of zinc in health and disease. Nat Rev Neurosci 2005;6:449.
[5] Bush AI, Pettingell WH, Multhaup G, Paradis M, Vonsattel JP, Gusella JF, et al. Rapid induction of Alzheimer A beta amyloid formation by zinc. Science 1994; 265:1464.
[6] Koh JY, Suh SW, Gwag BJ, He YY, Hsu CY, Choi DW. The role of zinc in selective neuronal death after transient global cerebral ischemia. Science 1996;272: 1013.
[7] Walker CF, Black RE. Zinc and the risk for infectious disease. Annu Rev Nutr 2004;24:255.
[8] Voegelin A, Poster S, Scheinost AC, Marcus MA, Kretzschmar R. Changes in zinc speciation in field soil after contamination with zinc oxide. Environ Sci Technol 2005;39:6616.

[9] Jiang P, Guo J. Fluorescent detection of zinc in biological systems: recent development on the design of chemosensors and biosensors. Coord Chem Rev 2004;248:205.
[10] Que EL, Domaille DW, Chang CJ. Metals in neurobiology: probing their chemistry and biology with molecular imaging. Chem Rev 2008;108:1517.
[11] Xu ZC, Yoon JY, Spring DR. Fluorescent chemosensors for Zn^{2+}. Chem Soc Rev 2010;39:1996.
[12] Lee VY, Sekiguchi A, Ichinohe M, Fukaya N. Stable aromatic compounds containing heavier group 14 elements. J Organomet Chem 2000;611:228.
[13] Hermanns J, Schmidt B. Five- and six-membered silicon–carbon heterocycles. Part 2. Synthetic modifications and applications of silacycles. J Chem Soc Perkin Trans 1999;1:81.
[14] Luo JD, Xie ZL, Lam JWY, Cheng L, Chen HY, Qiu CF, et al. Aggregation-induced emission of 1-methyl-1,2,3,4,5-pentaphenylsilole. Chem Commun 2001;1740.
[15] Tamao K, Uchida M, Izumizawa T, Furukawa K, Yamaguchi S. Silole derivatives as efficient electron transporting materials. J Am Chem Soc 1996;118:11974.
[16] Liu MS, Luo JD, Jen AKY. Efficient green-light-emitting diodes from silole-containing copolymers. Chem Mater 2003;15:3496.
[17] Toal SJ, Jones KA, Magde D, Trogler WC. Luminescent silole nanoparticles as chemoselective sensors for Cr(VI). J Am Chem Soc 2005;127:11661.
[18] Wang F, Luo J, Yang KX, Chen JW, Huang F, Cao Y. Conjugated fluorene and silole copolymers: synthesis, characterization, electronic transition, light emission, photovoltaic cell, and field effect hole mobility. Macromolecules 2005;38:2253.
[19] Ren Y, Lam JWY, Dong YQ, Tang BZ, Wong KS. Enhanced emission efficiency and excited state lifetime due to restricted intramolecular motion in silole aggregates. J Phys Chem B 2005;109:1135.
[20] Booker C, Wang X, Haroun S, Zhou J, Jennings M, Pagenkopf BL, et al. Tuning of electrogenerated silole chemiluminescence. Angew Chem Int Ed 2008;47:7731.
[21] Lu G, Usta H, Risko C, Wang L, Facchetti A, Ratner MA, et al. Synthesis, characterization, and transistor response of semiconducting silole polymers with substantial hole mobility and air stability: experiment and theory. J Am Chem Soc 2008;130:7670.
[22] Hou JH, Chen HY, Zhang SQ, Li G, Yang Y. Synthesis, characterization, and photovoltaic properties of a low band gap polymer based on silole-containing polythiophenes and 2,1,3-benzothiadiazole. J Am Chem Soc 2008;130:16144.
[23] Wang M, Zhang DQ, Zhang GX, Tang YL, Wang S, Zhu DB. Fluorescence turn-on detection of DNA and label-free fluorescence nuclease assay based on the aggregation-induced emission of silole. Anal Chem 2008;80:6443.
[24] Zhao MC, Wang M, Liu HJ, Liu DS, Zhang GX, Zhang DQ, et al. Continuous on-site label-free ATP fluorometric assay based on aggregation-induced emission of silole. Langmuir 2009;25:676.
[25] Hong YN, Lam JWY, Tang BZ. Aggregation-induced emission. Chem Sov Rev 2011;40:5361.
[26] Chu TY, Lu JP, Beaupré S, Zhang YG, Pouliot JR, Wakim S, et al. Bulk heterojunction solar cells using thieno[3,4-c]pyrrole-4,6-dione and dithieno[3,2-b:20,30-d]silole copolymer with a power conversion efficiency of 7.3%. J Am Chem Soc 2011;133:4250.
[27] Liu ZT, Xue WX, Cai ZX, Zhang GX, Zhang DQ. A facile and convenient fluorescence detection of gamma-ray radiation based on the aggregation-induced emission. J Mater Chem 2011;21:14487.
[28] Du XB, Wang ZY. Donor–acceptor type silole compounds with aggregation-induced deep-red emission enhancement: synthesis and application for significant intensification of near-infrared photoluminescence. Chem Commun 2011;47:4276.
[29] Song JS, Du C, Li CH, Bo ZS. Silole-containing polymers for high-efficiency polymer solar cells. J Polym Sci Part A 2011;49:4267.
[30] Hofmeier H, Schubert US. Recent developments in the supramolecular chemistry of terpyridine-metal complexes. Chem Soc Rev 2004;33:373.
[31] Wang F, Luo J, Chen JW, Huang F, Cao Y. Conjugated random and alternating 2,3,4,5-tetraphenylsilole-containing polyfluorenes: synthesis, characterization, strong solution photoluminescence, and light-emitting diodes. Polymer 2005;46:8422.
[32] Hong YN, Chen SJ, Leung CWT, Lam JWY, Liu JZ, Tseng NW, et al. Fluorogenic Zn(II) and chromogenic Fe(II) sensors based on terpyridine-substituted tetraphenylethenes with aggregation-induced emission characteristics. ACS Appl Mater Interfaces 2011;3:3411.